

HORIZONTAL TWO-PHASE FLOW PATTERN RECOGNITION

Original

HORIZONTAL TWO-PHASE FLOW PATTERN RECOGNITION / DE SALVE, Mario; Monni, Grazia; Panella, Bruno. - ELETTRONICO. - (2013), pp. 1-6. (8th World Conference on Experimental Heat Transfer, Fluid Mechanics and Thermodynamics Lisboa 16 – 20 June 2013).

Availability:

This version is available at: 11583/2513776 since:

Publisher:

Instituto Superior Técnico

Published

DOI:

Terms of use:

This article is made available under terms and conditions as specified in the corresponding bibliographic description in the repository

Publisher copyright

(Article begins on next page)

HORIZONTAL TWO-PHASE FLOW PATTERN RECOGNITION

Mario De Salve*, Grazia Monni* and Bruno Panella*

* Energy Department, Politecnico di Torino, C.so Duca degli Abruzzi 24, 10129 Turin, Italy
E-mail : grazia.monni@polito.it

ABSTRACT

In the present work a Wire Mesh Sensor (WMS) has been adopted to characterize the air-water two-phase flow in a test section consisting of a horizontal Plexiglas pipe of internal diameter 19.5 mm and total length of about 6 m. The flow quality ranges from 0 to 0.73 and the superficial velocity ranges from 0.145 to 31.94 m/s for air and from 0.019 to 2.62 m/s for water. The observed flow patterns are stratified-bubble-slug/plug-annular. The WMS consists of two planes of parallel wire grids (16x16) that are placed across the channel at 1.5 mm and span over the measuring cross section. The wires of both planes cross under an angle of 90°, with a diameter D_{wire} of 70 μm and a pitch equal to 1.3 mm. The void fraction profiles are derived from the sensor data and their evolution in time and space is analyzed and discussed. The dependence of the signals on the measured fluid dynamic quantities is discussed too. The main task is to predict which flow pattern will exist under any set of operating conditions as well as to predict the value of characteristic flow parameters.

Keywords : Horizontal Flow Pattern, Void Fraction Profiles

1. INTRODUCTION

The complexity of two phase flows is due to the existence of multiple, deformable and moving interfaces, and to significant discontinuities of the fluid properties across the interface, that lead to different spatial and temporal scales of the flow structure and state. The flow regimes are defined as the macro features concerning the multiphase interface structure and its distribution. In horizontal flow the effect of the gravity force contributes to the asymmetric distribution of the flow in the vertical direction.

The flow pattern is the result of the mechanical and thermal dynamic equilibrium between the phases, that depends on a large number of important parameters: the phases superficial velocity, the flow conditions (pressure and temperature), the fluid properties (density, viscosity, surface tension), the channel geometry and the flow direction (upward, downward, co-current, counter-current). A comprehensive classification of flow regimes in different pipe configuration and operating conditions is given by Rouhani and Sohal [1], Dobson et al. [2] and Thome [3].

A straight approach used to characterize the flow, is based on the measurement of the local void fraction and on the average cross-section or volumetric void fraction value. The void fraction can be measured by means of techniques like radiation attenuation (X or γ -ray or neutron beams) for line or area averaged values (Jones e Zuber [4]), optical (Bertola [5]) or electrical contact probes for local values, impedance techniques by using capacitance or conductance sensors (Prasser et al. [6]) and quick-closing valves based on the phases volume measurement.

The Wire Mesh Sensors (WMS), based on the measurement of the local instantaneous conductivity of the two-phase mixture, allows the evaluation of local void fraction, bubble size and phases velocity distributions. The WMS has been used, in different geometry and for different configurations, to study the

mean cross-section void fraction and gas profile evolution (Prasser et al. [7]). Comparative measurements between WMS and an X-ray tomography techniques have shown that the accuracy of the cross-section average void fraction depends on the two-phase flow pattern. Differences in the absolute void fraction were determined by Prasser et al. [8] for bubbly flows in the range of $\pm 1\%$, and for slug flows with an underestimation of approximately -4% . Da Silva et al. [9] have developed a WMS system based on permittivity (capacitance) measurements, which has been applied to investigate non-conducting fluids multiphase flows.

In the present work a WMS has been adopted to characterize the air-water two-phase flow in a horizontal Plexiglas tube ($D_i=19.5$ mm): local, chordal, cross-section void fraction values are derived from the sensor data and the flow evolution in time and space is analyzed and discussed. The dependence of the signals on the measured fluid dynamic quantities is discussed too. The main task is to estimate the flow pattern under any set of operating conditions, as well as to predict characteristic fluid and flow parameters (characteristic times, liquid levels, droplets distribution etc..) from the analysis of the void fraction chordal profiles that can be derived from the time history of the WMS signal.

2. WIRE MESH SENSOR

2.1 Geometry and Electronic Circuit

The sensor used in the present work has been constructed by Teletronic Rossendorf GmbH [8]. The sensor working principle is the measurement of the conductivity of the fluid. Because air and water have different electrical properties (water is high conductive while air is very low conductive) the measurement of the conductance can be analyzed to detect the presence of each

phase in the channel. The WMS (Fig. 1) consists of two planes of parallel wire grids (16x16) that are placed across the channel at a short distance from each other (1.5 mm); the wires of both planes cross under an angle of 90°. The sensor has been designed to cover the cross section of a channel having a 19.5 mm inner diameter; the wires have a diameter D_{wire} of 70 μm and a pitch p equal to 1.3 mm, so that only the 5.4% of the pipe section is occupied by the sensor. The measuring grid allows a spatial resolution of the order of the pitch length (1.3 mm) and it is possible to analyze the evolution of the investigated flow pattern, as the time resolution is rather high (up to 10.000 frames/s).

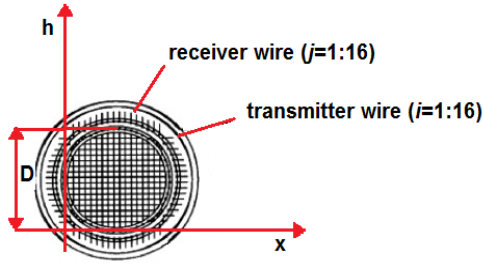


Fig. 1 Scheme of the WMS

2.2 Signal Processing

The WMS signals are acquired by means of WMS200 electronics and processed in Matlab® environment. The output is a 3-D matrix $V(i,j,k)$, where the indexes i and j are related with the space position of the mesh points and k is the time index, having a value between 1 and $T_T f_{acq}$, where T_T is the total observation time and f_{acq} is the acquisition frequency.

The value of $V(i,j,k)$ is a 12 bit digital signal proportional to the local fluid conductivity; the maximum value of the signal is 4079. The indexes i and j refer to transmitting wires and to receiving wires respectively. In order to analyze the signals, the location of the wires within the channel is defined: the points of the grid, that are located near the wall, are analyzed taking into account the wall influence, while the points, that are located outside the cross section of the pipe are excluded from the analysis. The developed signal processing scheme is structured to obtain the desired two-phase flow parameters.

First of all the signal is normalized taking into account the single phase reference matrix:

$$V^*(i, j, k) = \frac{V(i, j, k) - V_w(i, j)}{V_a(i, j) - V_w(i, j)} \quad (1)$$

where V_w and V_a are the time averaged values of the signals at the beginning of the test when the pipe is filled with water or air. The signal normalization can be considered as an approximation of the local void fraction value, if a linear relationship between conductivity and void fraction and a reference area equal to the square of the wire pitch p are assumed.

According to [9] slight overshoots and noise in the signal are corrected by:

$$V^*(i, j, k) = \begin{cases} 0 & V^*(i, j, k) \leq 0 \\ V^*(i, j, k) & 0 < V^*(i, j, k) < 1 \\ 1 & V^*(i, j, k) \geq 1 \end{cases} \quad (2)$$

From the evaluated local void fraction, the instantaneous chordal profiles are derived. The vertical profiles in the centre line of the pipe (index $j=8$) are used to evaluate the characteristic times and the characteristic shape of the void fraction profiles for the different flow conditions. The local instantaneous void fraction α has been obtained with an acquisition frequency f_{acq} equal to 1250 Hz for a total observation time T_T equal to 20 s.

The local void fraction in each point of the sensor grid is characterized by the signal histogram: the analysis of the normalized histograms, that are evaluated for the total observation time, allows us to define if a deterministic or a stochastic behavior characterizes the flow. The parameter σ/α_{mean} , where σ is the standard deviation of the signal and α_{mean} is the average void fraction is used as an index of the fluctuation of the signal. If a stochastic behavior is observed the mean value of the void fraction can be considered as representative of the flow, while in case of deterministic behavior further analysis is required. For non intermittent flows, the standard deviation value of the local void fraction is small, and the flow can be characterized with well defined void fraction profiles.

If the probability density function PDF is not a Gaussian curve and a quasi periodic behavior can be defined for the macroscopic structures of the flow, the characteristic times and the characteristic profiles have to be derived. In order to analyze fast phenomena in terms of average values, a moving average of the void fraction time values has been performed using a time interval τ .

Once the averaging time interval is defined, every average profile has been characterized from the statistical point of view by the root mean square profiles; while the variation in time of the chordal profile has been analyzed considering the evolution of the parameter $M(t)$ defined as the sum along the chord of the difference between the moving average local void fraction evaluated at the time t and at the time $t-\Delta t$:

$$M(t) = \sum_{i=1}^{16} (\langle \alpha(i, j, t) \rangle - \langle \alpha(i, j, t - \Delta t) \rangle) \quad (3)$$

where the corresponding time t is

$$t = \frac{k}{f_{acq}} \quad (4)$$

and Δt is equal to $1/f_{acq}$. Starting from the evolution in time of the $M(t)$ parameter it is possible to define the time interval in which the profile is constant and the time interval in which is evolving. The chordal profiles at the selected time are then analyzed and used to characterize the flow pattern in terms of time evolution and characteristic shape and parameters. A detailed description of the methodology can be found in reference [11].

3. FLOW PATTERN CHARACTERIZATION

In horizontal gas-liquid flows the flow can be classified in four general flow structures: stratified flow, bubbly flow, slug/plug flow and annular flow. Each flow pattern can be also divided in sub-categories: stratified flow in smooth and wavy flow, intermittent flow in slug and plug flow and annular flow in smooth, wavy and mist flow. Analyzing the macroscopic structure of the flow, for the different flow patterns, a characteristic shape of the void fraction vertical profile can be defined. The reference system is fixed in the bottom wall of the pipe with the coordinate h ranging from 0 to D , where D is the inner pipe diameter.

3.1 Stratified flow

A stratified flow is characterized by the complete separation of the two phases in gas and liquid streams, due to gravity effects. Liquid tends to flow along the bottom of the tube and gas along the top part. Qualitatively it is possible to distinguish between 3 regions: liquid region, interface region and gas region. The amplitude of the interface regions and the relative void profile depends on the amplitude of disturbance waves.

The vertical chordal profile is given by:

$$V^*_{i,j,k} = \begin{cases} 0 & h/D < h^* \\ 1 & h/D > h^* \end{cases} \quad (5)$$

$h^* \pm \Delta h^*$ is the position of the interface, where the local void fraction ranges from 0 to 1.

3.2 Bubbly flow

This flow pattern is characterized by the flow of bubbles, having the reference length (d_b) much smaller than the pipe diameter, dispersed in a continuous liquid phase. Due to the gravity effect, the bubbles tend to concentrate in the upper part of the pipe, so the local void fraction increases with h reaching the maximum in the upper half section of the pipe. If the bubble dimension is smaller than the distance between the measuring planes (1.5 mm), the local value of the void fraction is lower than one due to the simultaneous presence of gas and water in the measuring region. As the bubbles transit time is d_b/v_b (where v_b is the bubble velocity), the local void fraction changes with a frequency equal to the bubble frequency $f_b = d_b/v_b$.

3.3 Slug/Plug flow

The slug flow is characterized by a succession of slugs of liquids separated by large gas bubbles whose diameter approaches that of the pipe. The slug unit consist of the slug body, having a length L_s , and a stratified region (or bubble region) having a length L_b . The slug body propagates along the pipe with a velocity v_s higher than the film velocity producing an entrainment of gas from the film region to the slug body (aeration). As the structure of the slug flow is almost identical to that of plug flow, the two regimes are classified as an unique

flow pattern, the so called "intermittent" flow. For the slug and the plug flow, due to the intrinsically intermittent nature of the flow, the modeling of the void fraction vertical profile requires consideration about the transit times and the shapes of slugs and plugs/bubbles. Two profiles, related with the two characteristic time $\tau_s = L_s/v_s$, $\tau_b = L_b/v_b$ can be defined, considering that $\tau_{tot} = (\tau_s + \tau_b) = (L_s + L_b)/J_{tot}$, where J_{tot} is the total areal velocity of the flow.

3.4 Annular flow

An annular flow is characterized by the presence of a continuous liquid film at the wall surrounded by a central gas core (gas continuous phase) containing a varying amount of entrained liquid droplets (liquid dispersed phase). The flow is symmetric with respect to the vertical pipe axis; while the liquid film strongly depends on the superficial velocities of the phases and is asymmetric due to the gravity effect in horizontal flow. Under the hypothesis of fully developed flow, it is theoretically possible to define the liquid film region, the interface region and the core region. The void fraction in the core region can be different from one, depending on the reached equilibrium between the drops entrainment and deposition rate.

4. EXPERIMENTAL FACILITY AND TEST MATRIX

The experimental facility consists of the feed water loop (tap water with conductivity of about 620 μS is used), the feed air loop and the test section. The liquid flow rate is measured with a $\pm 0.5\%$ r.v. accuracy value. The air flow rate is measured by means of different rotameters for the different ranges with a $\pm 2\%$ f.s.v. accuracy value. The test section consists of a 19.5 mm diameter and about 6 m long horizontal pipe. The WMS is located between two Plexiglas pipes having a length of 600 mm. Experiments have been performed at water temperature of about 20 °C. The flow quality ranges from 0 to 0.73 and the superficial velocity ranges from 0.14 to 31.94 m/s for air and from 0.019 to 2.62 m/s for water. The pressure ranges from atmospheric pressure to 3.7 bar depending on the experimental conditions. The typical observed flow patterns are stratified flow, intermittent flow (slug and plug) and non symmetric annular flow. The population of samples is more representative of intermittent and annular wavy regimes. The comparison between the observed flow patterns and the prediction by the Baker's and the Mandhane's maps is reported in Fig. 2: the flows are identified by superficial velocities (J_g , J_l). Some runs have been performed in transition regimes on the ground of the visual observation and maps results.

5. EXPERIMENTAL DATA ANALYSIS

In order to analyze the chordal profiles, the different time and space scales of the two phase flow have to be evaluated. A fundamental task for the flow analysis is then the choice of the signal acquisition frequency and of the observation time. A high acquisition frequency allows the detection of the fast transient phenomena while a long observation time allows the detection of the slow phenomena. In the present work we focus the attention

on the macroscopic flow objects (like plug, slug, bubbles, droplets, waves). The adopted acquisition frequency (1250 Hz) is sufficient to detect and characterize objects having a minimum space length equal to $L_{min}=2 \cdot v_{max}/f_{acq}$. Because the flow velocity ranges from 0.26 m/s to 32 m/s, the minimum length at lower velocities is of the order of 0.5 mm, while at the highest velocity can reach 50 mm. The selected observation period (20 s) allows the analysis of the phenomena having a characteristic frequency higher than 0.1 Hz.

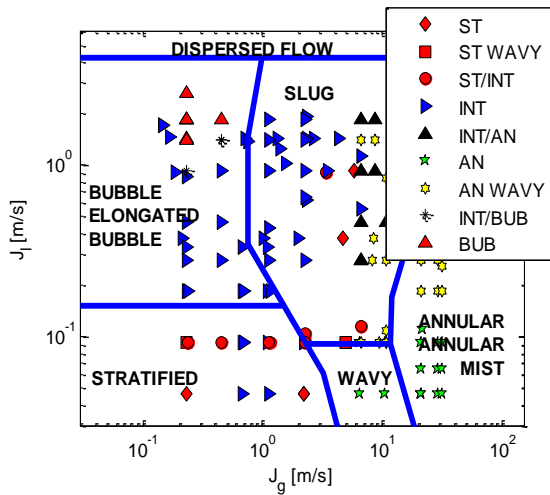


Fig. 2 Comparison between Mandhane's Map flow patterns prediction and observations. Legend: ST=Stratified, INT=Intermittent, AN=Annular, BUB=Bubble

5.1 Void fraction chordal profile

The void profiles corresponding to $j=8$ are reported for selected cases in order to evaluate the influence of the phases velocity during the time flow evolution and the phases distribution. In order to obtain a characteristic shape of the flow that can be related to the superficial flow velocity the moving average profiles have been evaluated. In Fig. 3 the time evolution of the parameter $M(t)$, obtained using a moving average time τ of 0.4 s, is plotted for different air and water superficial velocities. The optimum time interval, used for the moving average profiles, has been selected as the minimum averaging time, that allows us to maximize the time period in which $M(t)$ is zero. The time history of $M(t)$ is strongly dependent on the superficial velocities for both frequency and amplitude, so it is possible to extract the profiles that characterize the flow for different time periods.

If the amplitude is lower than a threshold value the flow can be characterized by the mean profile and the correspondent standard deviation (Fig. 3 (a)), and it is classified as “non intermittent” or “non periodic profile” flow; while for higher amplitudes, ($M(t)$ higher than 0.1 in absolute value) a number of profiles depending on the time history have to be analyzed. In this case the flow evolution can be divided in two categories “quasi periodic profile” (Fig. 3 (b)), and “non periodic profile with high noise” (Fig. 3 (c)): the profile is classified as “quasi periodic” if there is a time period in which the profile doesn't change significantly, while it is classified as “non periodic high

noise” if the absolute value of $M(t)$ is higher than the threshold value and the local flow is characterized by a chaotic behavior. For the “high noise” profile, in which the value of the $M(t)$ is continuously changing, the time evolution is characterized by the mean profile, that is evaluated adopting the observation time of 20s, and by the relative standard deviation.

For the “quasi periodic” profile at least two characteristic profiles with the related time are derived considering the time periods in which $M(t)$ is near zero and the time periods in which the flow is evolving and $M(t)$ is higher than zero.

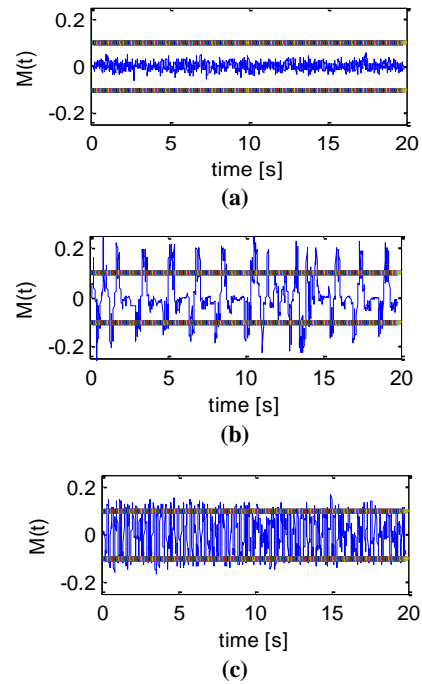


Fig. 3 $M(t)$ time evolution at $j=8$. (a) $J_g=0.23$ m/s - $J_1=1.86$ m/s, (b) $J_g=2.26$ m/s - $J_1=0.65$ m/s, (c) $J_g=8.73$ m/s - $J_1=1.86$ m/s

For classification purpose and considering the time interval that has been adopted to perform the moving average, the limit value has been considered of the order of 0.5 s: the profile is considered as “quasi periodic” if the profile doesn't change significantly for a period higher than 0.5 s. If the water superficial velocity (J_1) is lower than 0.5 m/s and the air superficial velocity (J_g) is lower than 10 m/s the profile evolution is characterized by a quasi periodic behavior; if the air velocity is increased up to values higher than 10 m/s and the water velocity values are lower than 0.5 m/s, the amplitudes related with the profile change evolution parameters are lower than the threshold value and then the flow can be characterized by a single profile shape. If the value of the air velocity is lower than 10 m/s and the water velocity is higher than 0.5 m/s the evolution of the $M(t)$ is characterized by a high noise and by an amplitude higher than the threshold value; but for a water velocity further increase the amplitude tends to decrease and an amplitude lower than 0.1 has been detected for water superficial velocities higher than 1.4 m/s and air superficial velocities lower than 0.5 m/s.

5.2 Analysis of the void fraction profiles

From the analysis of the $M(t)$ time evolution, the flow characteristic profiles are derived and qualified in terms of shape and flow parameters. In Fig. 4 the characteristic void fraction chordal profile is shown for two different flows, characterized by low amplitude values of $M(t)$. In Fig. 4 (a) the typical profile of an horizontal bubbly flow is shown, while in Fig. 4 (b) the flow can be classified as annular.

Considering the flow of Fig. 4 (a), the parameters that have to be defined in order to classify it are: the height of the stratified region, the mean value of the void fraction in the bubbles region, the mean value of the void fraction in the stratified region and the related standard deviation, and finally the mean value of the void fraction in the upper part of the pipe, close to the wall.

For the annular flow shown in Fig. 4 (b), in order to qualify it, the parameters like the liquid film thickness, the interface position, the void fraction in the core region have to be quantified.

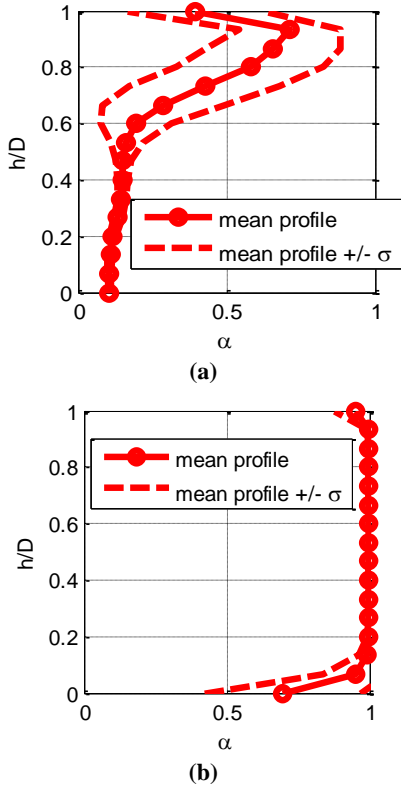


Fig. 4 Characteristic void fraction chordal profile for non-intermittent flows. (a) $J_g=0.23$ m/s – $J_l=1.86$ m/s, (b) $J_g=29.3$ m/s – $J_l=0.05$ m/s

The frequency spectrum of the flows classified also as “non periodic with low noise”, that is evaluated in points of the grid representative of the flow (Fig. 5), shows that the energy of the signal is different along the chord, but a predominant characteristic frequency is not observed.

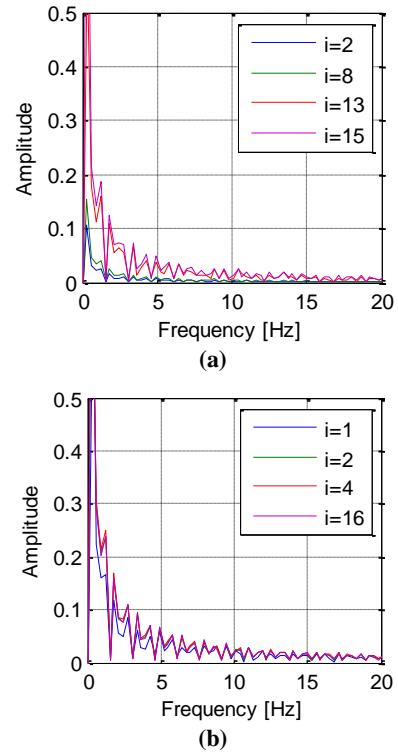


Fig. 5 Frequency spectrum at $j=8$ for non-intermittent flows. (a) $J_g=0.23$ m/s – $J_l=1.86$ m/s, (b) $J_g=29.3$ m/s – $J_l=0.05$ m/s

If the flow is fast intermittent or “non periodic with high noise” (Fig. 6) the stochastic/deterministic behavior of the profile change is analyzed by means of the probability density function in each measuring point of the chord: the mean profile, the standard deviation profile and the time period are derived. Then the profile is characterized in terms of shape parameters and in terms of their oscillation amplitudes. The characteristic profile is calculated as the mean time profile (Fig. 6).

For flow classified as “non periodic with high noise”, the frequency spectrum shows the presence of characteristic frequencies in the range between 20 and 40 Hz as in the case analyzed in Fig. 7.

If the flow is classified as “quasi-periodic” (Fig. 8), the profile evolution during the two characteristic periods (absolute value of $M(t)$ higher than zero or near zero) is analyzed. The changing profile period is analyzed, in terms of profile evolution (profiles at $M(t)$ min and max and corresponding times), while the mean profile and the variation amplitude are used for the second period. The flow is then described at least by two characteristic profiles and by the characteristic time of each one. This flow is typical of intermittent flows, such as slug flow. The red line (diamonds) refers to the slug region profile, while the blue line (circles) refers to the bubble region profile of the slug unit; the dashed lines represent the $(\alpha_{\text{mean}} \pm \sigma)$ profile; in Fig. 8 it is also reported the slug and bubble total residence time.

The characteristic frequencies are in the range between 0 and 20 Hz, as shown in Fig. 9.

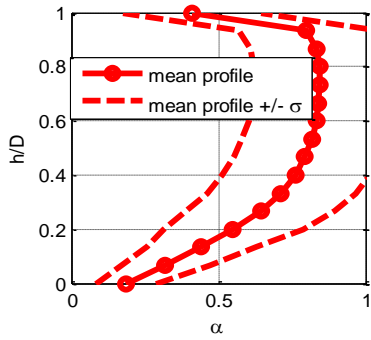


Fig. 6 Profiles analysis for “non periodic with high noise” flow at $J_l=1.86$ m/s - $J_g=8.73$ m/s

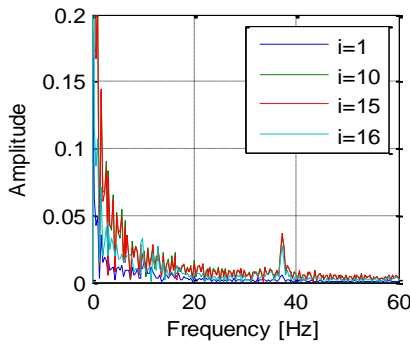


Fig. 7 Frequency spectrum at $j=8$ for $J_l=1.86$ m/s - $J_g=8.73$ m/s

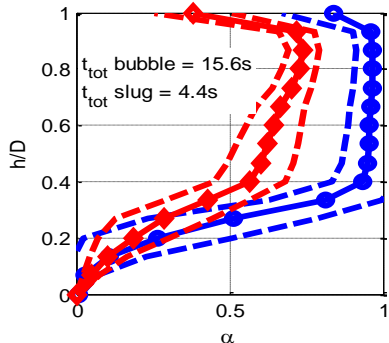


Fig. 8 Profiles analysis for the “quasi periodic” flows at $J_l=0.65$ m/s - $J_g=2.26$ m/s

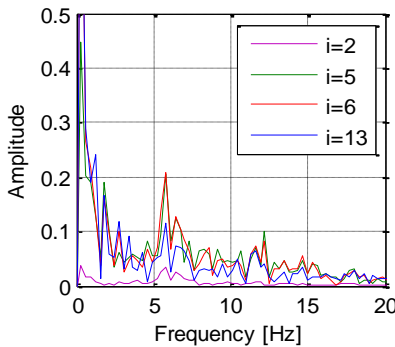


Fig. 9 Frequency spectrum at $j=8$ for $J_l=0.65$ m/s - $J_g=2.26$ m/s

5.3 Profile shape dependence on phases velocity

In the following figures the dependence of the shape profile on the phases velocity is analyzed for the flows that are classified as “quasi periodic”: two characteristic void fraction profiles, corresponding to the slug and bubble regions, are analyzed as a function of the ratio J_g/J_l (Fig. 10). Concerning the slug region profiles, the effect of the liquid velocity increase is the reduction of the peak of the void fraction profile, and the tendency to a more homogeneous chordal profile, while the effect of the air rate increase is the reduction of the stratified region thickness due to the entrainment of bubbles within the upper region. The bubble region is characterized by a stratified liquid thickness that decreases by increasing the air velocity; a thin liquid film in the upper region of the channel with a thickness that increases with the liquid flow rate is detected by the sensor. The value of the void fraction in the bubble region approaches unity at the lowest water velocities, but tends to decrease at water velocity higher than 0.8 m/s.

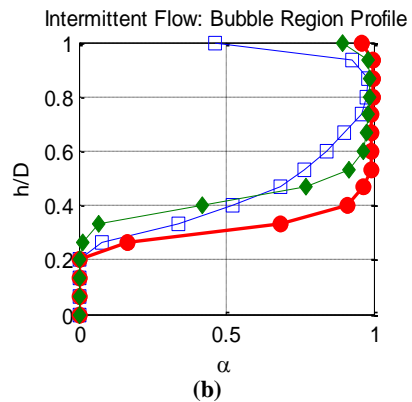
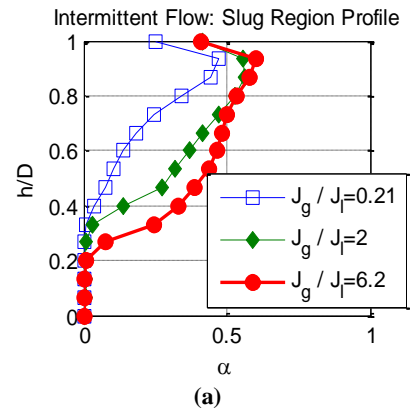


Fig. 10 “Quasi periodic” flow profiles dependence on the ratio J_g/J_l

In the following figures the velocity dependence of the characteristic profiles for the flows that can be classified as “non periodic with low noise” and “non periodic with high noise” is shown. Fig. 11 presents the profile evolution that is obtained by increasing the liquid flow rate, at three air flow rates (2.33 m/s, 11 m/s, 21.21 m/s). At lower air velocity and at water velocity lower than 2 m/s the profiles show a peaked shape, with the peak

localized in the upper region of the pipe where the gas phase is concentrated due to the gravity force. By increasing the air flow rate the flow tends to become more symmetric with respect to the pipe center and the typical shape of an annular flow is reached.

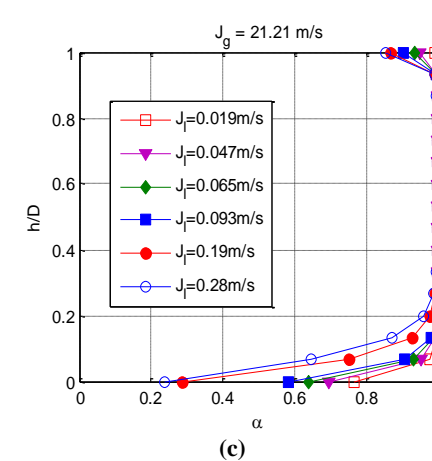
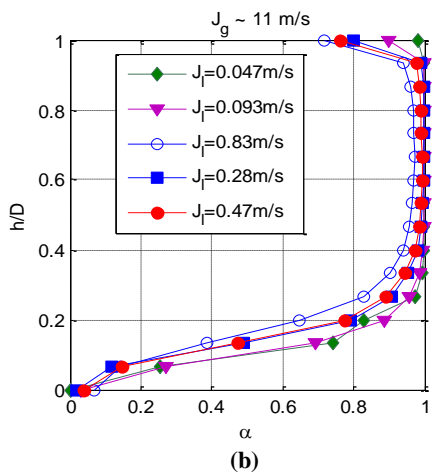
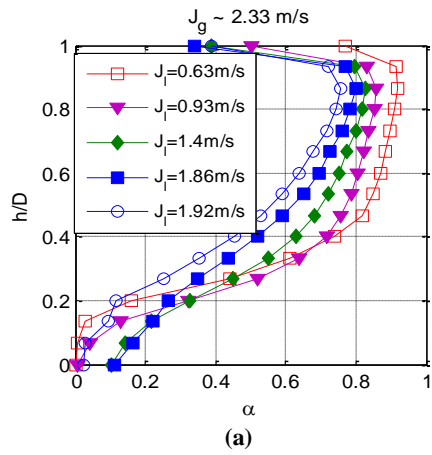


Fig. 11 Void fraction profile at different air velocity:
(a) $J_g=2.33$ m/s, (b) $J_g=11$ m/s, (c) $J_g=21.21$ m/s

At air velocities ranging from 4 m/s to 10 m/s the liquid entrainment in the core region is detected and the thickness of the liquid film either in the upper cross section region or at bottom is higher (Fig. 11 (b), Fig. 12 (b) and (c)). In Fig. 12 the profiles at three water velocities (0.09 m/s, 0.93 m/s and 1.86 m/s) and at

different air velocity are presented: at lower water velocity the characteristic shape is reported in Fig. 12 (a): stratified and annular flows occur with a liquid film thickness that decreases by increasing the air flow rate.

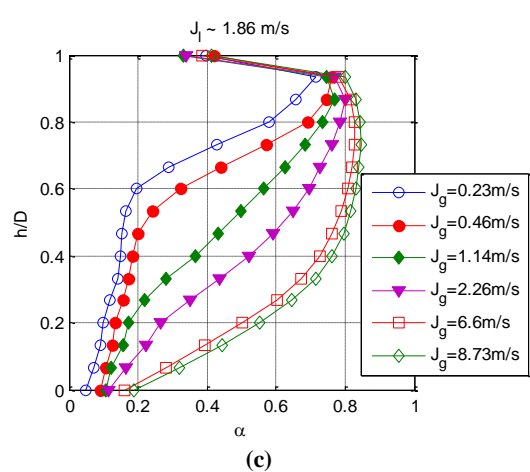
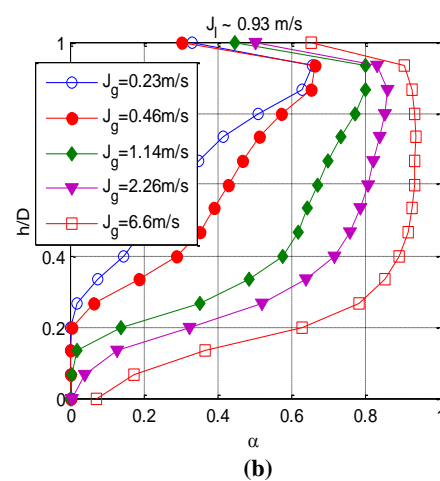
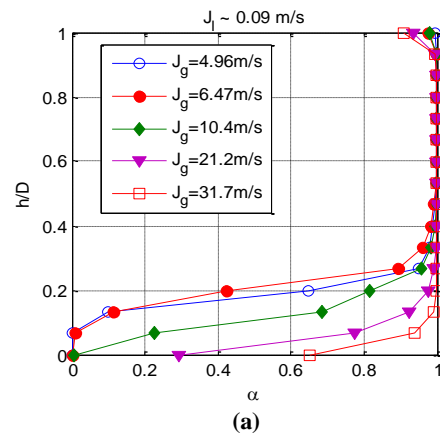


Fig. 12 Void fraction profile at different water velocity:
(a) $J_l=0.09$ m/s, (b) $J_l=0.93$ m/s, (c) $J_l=1.86$ m/s

At higher water velocity the evolution from bubble flow to annular flow is shown in Fig. 12 (b and c); the air flow rate increase produces an increase of the void fraction, reduces the liquid film thickness both in the upper and lower region of the pipe: it tends to flat the profile in the central region, resulting in a

more symmetric profile. At higher water velocity (Fig. 12 (c)) the upper liquid film region seems to be unaffected by the air flow rate, while the void fraction value in the lower region is higher than the liquid reference value ($\alpha=0$), due to the air that is entrained inside the liquid film.

The profiles that are obtained for bubble flow allows some important considerations: the bubble flow is characterized, for the present test conditions, by a void fraction distribution that strongly depends on the gravity force (peaked profile) and the maximum value of the void fraction along the chord is reached near the channel top and ranges from about 0.4 to 0.75 depending on the phases velocity combination. A liquid film in the cross section upper region has been detected by the sensor for all the tested flow conditions.

If the liquid velocity increases the flow tends to homogenize with a void fraction at the channel bottom higher than zero while the maximum void fraction value decreases. By increasing the air velocity the mean chordal void fraction increases and the profile flattens evolving in annular flow. The transition to the annular flow seems to coincide with a translation of the void fraction maximum value towards the centre of the pipe. Where the air velocity is lower than 11 m/s the core region of the annular flow is characterized by a value of the void fraction lower than one, while at higher velocity the value is zero.

CONCLUSIONS

Air-water experiments have been performed in a horizontal Plexiglas pipe, having an internal diameter of 19.5 mm and a total length of about 6 m. The superficial velocities of the two phases range from 0.14 to 32 m/s for air and from 0.019 to 2.62 m/s for water. In the present work a WMS has been adopted to characterize the air-water two-phase flow: local, chordal, cross-section void fraction values are derived from the sensor data.

The developed methodology for the analysis of the signals allows the identification of the flow pattern and the flow characterization in terms of void fraction profiles and characteristic times. From the analysis of the time evolution of the local void fraction and of the parameter $M(t)$ it is possible to characterize the flow in terms of the void fraction profile shape and other parameters like phases distribution, liquid level, mean void fraction in the different pipe region, characteristic frequencies.

The evolution of the void fraction profiles has been related to the superficial velocity of the two phases (J_g and J_l) and the flow evolution in time and space has been analyzed and discussed.

ACKNOWLEDGEMENTS

The present research has been supported by ENEA and by the Ministry of Economic Development. The authors thank Rocco Costantino and Giuseppe Vannelli for the support through their work.

REFERENCES

1. S.Z. Rouhani and M S Sohal, Two-Phase Flow Patterns: A Review of Research Results, *Progress in Nuclear Energy*, Vol. 11, No. 3, pp. 21~259, 1982.
2. M.K. Dobson, Heat transfer and flow regimes during condensation in horizontal tubes, Ph.D. Thesis, University of Illinois, Urbana, IL, 1994.
3. J. Thome Engineering Data Book III, *WolverineTube INC.*, 2004.
4. Jr. O.C Jones, and N. Zuber, The interrelation between void fraction fluctuations and flow patterns in two-phase flow. *Int. J. Multiphase Flow*, 2, 273-306, 1975.
5. V. Bertola, Experimental characterization of gas-liquid intermittent subregimes by phase density function measurement, *Experiments in Fluids* 34 122-129, 2003.
6. H.M. Prasser, A. Böttger, J. Zschau, A new electrode-mesh tomograph for gas-liquid flows, *Flow Measurement and Instrumentation*, 9 111-9, 1998.
7. H.M. Prasser, E. Krepper, D. Lucas, Evolution of the two-phase flow in a vertical tube-decomposition of gas fraction profiles according to bubble size classes using WMSs, *Int. J. Therm. Sci.*, 41 17-28, 2002.
8. H.M. Prasser, M. Misawa and I. Tiseanu, Comparison between wire-mesh sensor and ultra-fast X-ray tomography for an air-water flow in a vertical pipe, *Flow Meas. and Instr.*, Vol. 16, 73-83, 2005.
9. M.J. Da Silva, E. Schleicher, and U. Hampel, Capacitance wire-mesh sensor for fast measurement of phase fraction distributions, *Meas. Science and Tech.*, Vol. 18, 2245-2251, 2007.
10. Teletronic Rossendorf GmbH, Wire Mesh Sensor System, WMS200 Manual, Version 1.2, 2010.
11. M. De Salve, G. Monni, B. Panella, Horizontal Air -Water Flow Pattern Recognition, to be presented to the Wessex 2013 *Multiphase Flow Conference*, 2013.